The American Journal of Pathology, Vol. 172, No. 5, May 2008

DOI: 10.2353/ajpath.2008.070207

Cardiovascular, Pulmonary and Renal Pathology

Interleukin-13 Protects Against Experimental Autoimmune Myocarditis by Regulating Macrophage Differentiation

Daniela Cihakova,* Jobert G. Barin,*† Marina Afanasyeva,‡ Miho Kimura,* DeLisa Fairweather,*§ Michael Berg,¶ Monica V. Talor,* G. Christian Baldeviano,¶ Sylvia Frisancho,§ Kathleen Gabrielson,‖ Djahida Bedja,‖ and Noel R. Rose*¶

From the Departments of Pathology, and Molecular and Comparative Pathobiology,‖ and the Graduate Program in Immunology,† The Johns Hopkins University School of Medicine, Baltimore, Maryland; the W. Harry Feinstone Department of Molecular Microbiology and Immunology,¶ and the Department of Environmental Health Sciences,§ the Johns Hopkins University Bloomberg School of Public Health, Baltimore, Maryland; and the Cardiovascular Research Group,‡ Faculty of Medicine, University of Calgary, Calgary, Canada*

We report here that interleukin (IL)-13 protects BALB/c mice from myocarditis, whether induced by peptide immunization or by viral infection. In contrast to mild disease in IL-4 knockout (KO) BALB/c mice, IL-13 KO BALB/c mice developed severe coxsackievirus B3 (CVB3)-induced autoimmune myocarditis and myocarditogenic peptide-induced experimental autoimmune myocarditis. Such severe disease was characterized by increased cardiac inflammation, increased total intracardiac CD45$^+$ leukocytes, elevated anti-cardiac myosin autoantibodies, and increased cardiac fibrosis. Echocardiography revealed that IL-13 KO mice developed severe dilated cardiomyopathy with impaired cardiac function and heart failure. Hearts of IL-13 KO mice had increased levels of the proinflammatory and profibrotic cytokines IL-1β, IL-18, interferon-γ, transforming growth factor-β1, and IL-4 as well as histamine. The hallmark of the disease in IL-13 KO mice was the up-regulation of T-cell responses. CD4$^+$ T cells were increased in IL-13 KO hearts both proportionally and in absolute number. Splenic T cells from IL-13 KO mice were highly activated, and myosin stimulation additionally increased T-cell proliferation. CD4$^+$CD25$^+$Foxp3$^+$ regulatory T-cell numbers were decreased in the spleens of IL-13 KO mice. IL-13 deficiency led to decreased levels of alternatively activated CD206$^+$ and CD204$^+$ macrophages and increased levels of classically activated macrophages. IL-13 KO mice had increased caspase-1 activation, leading to increased production of both IL-1β and IL-18. Therefore, IL-13 protects against myocarditis by modulating monocyte/macrophage populations and by regulating their function. ***(Am J Pathol 2008, 172:1195–1208; DOI: 10.2353/ajpath.2008.070207)***

Idiopathic cardiomyopathy of nonischemic origin is often preceded by myocarditis and represents an increasing public health problem.[1,2] Similar to the human disease, infection of mice with coxsackievirus B3 (CVB3) results in the development of an acute, self-limited myocarditis in a majority of mice, but a few genetically susceptible strains proceed to autoimmune myocarditis and dilated cardiomyopathy (DCM) by day 35 after infection.[3,4] Cardiac myosin heavy chain is a major target of autoimmune responses in CVB3-induced myocarditis.[5] Immunization with cardiac myosin purified from murine hearts or cardiac myosin heavy chain peptide in complete Freund's adjuvant can induce experimental autoimmune myocarditis (EAM).[6–8] Both cell-mediated and antibody-mediated immunity contribute to the final pathological picture of chronic inflammation and DCM in EAM and CVB3-induced myocarditis.[9,10]

We previously demonstrated that EAM in A/J mice carry hallmarks of Th2-like pathology. Blockade of interleukin (IL)-4 partially suppresses the development of EAM, indicating that IL-4 is cardiopathogenic in this strain.[9] The importance of IL-4 in the pathogenesis of EAM suggests that other Th2 cytokines could also augment EAM pathology. Therefore, we postulated that IL-13, another Th2 cytokine,

Supported by the National Institutes of Health (National Heart, Lung, and Blood Institute grants R01 HL70729, R01 HL67290, and HL087033).

Accepted for publication February 5, 2008.

Supplemental material for this article can be found on *http://ajp.amjpathol.org*.

Address reprint requests to Daniela Cihakova, M.D., Ph.D., Johns Hopkins University, Department of Pathology, Division of Immunology, Ross 648, 720 Rutland Ave., Baltimore, MD 21205. E-mail: dcihako1@jhmi.edu.

could synergize with IL-4, and that IL-13 knockout (KO) mice would develop reduced EAM and CVB3-induced myocarditis. However, our unexpected results presented in this article have led to the novel conclusion that IL-13 exerts protective effects in this autoimmune disease.

IL-13 is a pleiotropic cytokine produced by T-helper-type 2 (Th2) $CD4^+$ T cells, $CD8^+$ T cells, mast cells, dendritic cells, and eosinophils.[11,12] IL-13 does not use the classical receptor for IL-4 (IL-4Rα/γ_c), but shares use of the alternative IL-4 receptor, consisting of IL-4Rα and the IL-13 receptor α1 (IL-13Rα1) subunit.[13] In addition to the common receptor with IL-4, IL-13 has an additional receptor: IL-13Rα2, which possesses antagonistic decoy functions, in addition to unique signaling functions.[14] There is growing evidence of unique physiological functions of IL-13, not shared by IL-4, in models of helminthic parasitism,[15,16] schistosomiasis,[17,18] lung immunity and atopy,[19,20] and tumor immunity.[21]

T cells are not known to express functional IL-13Rα1 and so IL-13 is probably not directly acting on T cells. The main targets of IL-13 are monocytes/macrophages. IL-13 signaling in monocytes yielded a transcriptional profile unique and distinct from macrophages classically activated by interferon (IFN)-γ. IL-13 and IL-4 alternatively activated macrophages show distinct phenotypic changes: mannose receptor up-regulation, induction of selective chemokines, and expression of arginase. Also, IL-13 prevents lipopolysaccharide-dependent caspase-1 activity in monocytes, therefore decreasing production of IL-1 and IL-18. This role of IL-13 on macrophages contrasts with the activation of macrophages by IFN-γ: up-regulation of iNOS, as well as the proinflammatory cytokines IL-6, tumor necrosis factor (TNF)-α, and IL-1.[22,23]

We report here that IL-13 KO mice on a BALB/c background developed significantly increased myosin- and CVB3-induced myocarditis. IL-13 reduces myocarditis by regulating monocyte/macrophage populations during EAM.

Materials and Methods

Mice

IL-13 KO and IL-13/IL-4 DKO mice on the BALB/c background were generated in the laboratory of Andrew McKenzie, as described[15,18] and were bred and maintained in the Johns Hopkins University School of Medicine conventional animal facility. IL-4 KO and WT BALB/c mice were obtained from the Jackson Laboratory (Bar Harbor, ME) and maintained in the Johns Hopkins University School of Medicine conventional animal facility. All experiments were conducted on 6- to 8-week-old male mice. All methods and protocols involving mice were approved by the Animal Care and Use Committee of the Johns Hopkins University.

Induction of EAM

For the induction of EAM, we used the myocarditogenic peptide MyHC$\alpha_{614-629}$ derived from the sequence of the murine cardiac myosin heavy chain (Ac-SLKLMATLFSTYASAD-OH)[8,24] commercially synthesized by fMOC chemistry and purified by high performance liquid chromatography (Global Peptide, Fort Collins, CO). On days 0 and 7, mice received subcutaneous injections of 200 μg of MyHC$\alpha_{614-629}$ peptide emulsified in complete Freund's adjuvant (Sigma, St. Louis, MO) supplemented with 5 mg/ml of *Mycobacterium tuberculosis*, strain H37Ra (Difco, Detroit, MI). On day 0, mice additionally received 500 ng of pertussis toxin intraperitoneally (List Biologicals, Campbell, CA). For CVB3-induced myocarditis, IL-13 KO and WT BALB/c mice were inoculated intraperitoneally with 10^3 plaque-forming units of a heart-passaged stock of CVB3 (Nancy strain), originally obtained from the American Type Culture Collection (Manassas, VA), diluted in sterile phosphate-buffered saline (PBS) on day 0. Individual experiments were conducted at least three times with 7 to 10 mice per group.

Histopathology

Mice were evaluated for the development of EAM at the peak of disease on day 21 or in chronic stage of EAM at day 30 or chronic CVB3-induced myocarditis at day 35 after infection. Heart tissues were fixed in 10% phosphate-buffered formalin. Five-μm sections were cut longitudinally and stained with hematoxylin and eosin, and Masson's trichrome for fibrosis. Myocarditis severity was evaluated by histopathological microscopic approximation of the percent area of myocardium infiltrated with mononuclear cells or fibrosis determined from five sections per heart according to the following scoring system: grade 0, no inflammation; grade 1, less than 10% of the heart section is involved; grade 2, 10 to 30%; grade 3, 30 to 50%; grade 4, 50 to 90%; grade 5, more then 90%. For CVB3-induced myocarditis the severity of the disease was assessed as the percentage of the heart section with inflammation compared with the overall size of the heart section, with the aid of a microscope eyepiece grid. Two independent researchers scored slides separately in a blinded manner.

Antibodies to Cardiac Myosin

Mice were bled on days 0 and 21 from the retro-orbital venous plexus using heparinized capillary tubes. Sera were collected by heart puncture on day 35 after infection of CVB3-induced myocarditis. Serum levels of MyHC$\alpha_{614-629}$-reactive (EAM) or cardiac myosin (CVB3) antibodies were determined using microtiter plates coated with 0.5 μg of MyHC$\alpha_{614-629}$ or cardiac myosin incubated with phosphatase-conjugated isotype-specific secondary antibodies. Adjusted optical density (OD) was calculated as follows: adjusted OD = mean OD of a sample − mean OD of a negative control. The autoantibody titer is expressed as the reciprocal of the highest serum dilution having an OD greater than that of the negative control serum plus three SD. Negative control serum consisted of pooled sera from 10 uninfected BALB/c mice.

Cytokine, Histamine, and Caspase-1 Enzyme-Linked Immunosorbent Assay (ELISA)

Half of the heart or spleen was snap-frozen on dry ice immediately after resection and stored at −80°C until homogenized in minimal essential medium plus 2% fetal bovine serum, debris cleared by centrifugation, and stored at −80°C until used in ELISA. Cytokine levels were measured in homogenized heart and spleen supernatants using Quantikine cytokine ELISA kits (R&D Systems, Minneapolis, MN), according to the manufacturer's instructions. The limit of detection for the cytokine kits were as follows: IFN-γ, 2 pg/ml; transforming growth factor (TGF)-β1, 1.6 pg/ml; IL-1β, 3 pg/ml; IL-4, 2 pg/ml; IL-13, 1.5 pg/ml; IL-17, 5 pg/ml; IL-18, 25 pg/ml; histamine, 1.5 ng/ml. Heart cytokine and histamine levels were expressed as pg/g of heart tissue. Caspase-1 activity was measured from 5×10^6 splenocytes from IL-13 KO mice on day 21 of EAM. Splenocytes were snap-frozen and stored at −80°C until caspase-1 activity was measured. Caspase-1 activity was measured by the Casp-1/ICE fluorometric assay kit (BioVision, Mountain View, CA).

In Vitro *MyHC$\alpha_{614-629}$-Specific Proliferation*

Single cell suspension was prepared from mice spleens. After enumeration in a hemocytometer and standardization of cell densities in RPMI 1640 and 10% fetal bovine serum, 2.5×10^5 responder cells were plated with 10 μg/ml of MyHC$\alpha_{614-629}$ in triplicate in 96-well format. Control cells were cultured with media in the absence of MyHC$\alpha_{614-629}$. All cells were incubated at 37°C, 5% CO_2 for 48 hours. Proliferation assay plates were pulsed 24 hours before harvest with 1 μCi/well [^{3}H]-methyl thymidine (GE Amersham, Buckinghamshire, UK), harvested onto glass filters, and specific radio-uptake detected on a Trilux β-direct counter (Packard, Waltham, MA).

Flow Cytometry

The heart was perfused at a constant flow of 14 ml/minute with cold PBS (Biofluids, Carlsbad, CA) for 2 minutes, and then digested with collagenase II (100 μg/ml; Sigma-Aldrich, St. Louis, MO) and protease XIV (50 μg/ml; Sigma-Aldrich) in PBS for 7 minutes at 37°C.[25,26] After careful mincing, single cell suspensions were sequentially passed through 70-μm and 40-μm cell strainers (BD Falcon, Franklin Lakes, NJ). Splenocytes were also extracted into single cell suspension in 1× PBS, and red blood cells lysed by incubation in ACK lysis buffer (Biofluids). Cells were washed and FcγRII/III blocked with αCD16/32 (eBiosciences, San Diego, CA). Surface markers were stained with fluorochrome-conjugated mAbs to CD3ε, CD4, CD8α, CD11b (Mac1), CD11c, CD19, CD25, CD28, CD44, CD45, CD45R (B220), CD62L, CD69, CD71, CD80 (B7.1), CD86 (B7.2), CD117 (c-kit), CD152 (CTLA4), CD204 (SR-A), CD206 (MR), CD274 (PD-L1), DX5, F4/80, FcεRIα, Gr1 (Ly6G), Mac3, MHC Class II (I-A/I-E), and TCRβ (eBiosciences; BD Pharmingen, San Diego, CA; Biolegend, San Diego, CA; and AbD Serotec, Raleigh, NC). Treg cells were further stained by intracellular staining of Foxp3 with a kit according to manufacturer's instructions (eBiosciences). Samples were acquired on a four-color dual-laser FACScalibur cytometer running the CellQuest software package or the LSR II quad-laser cytometer running FACS-Diva (BD Immunocytometry, San Jose, CA).

Echocardiography

Trans-thoracic echocardiography was performed using the visualsonic Vevo 660 imaging system equipped with a 40 MHz transducer (VisualSonics Inc., Toronto, Canada). Conscious, previously trained mice were gently held in a supine position in the palm of the hand, as described.[25,27] The left hemi-thorax was shaved and ultrasonic transmission gel (Parker Laboratories, Fairfield, NJ) was applied to the thorax. The heart was imaged in the two-dimensional mode in the parasternal short axis view. From this mode, an M-mode cursor was positioned perpendicular to the interventricular septum (IVS) and the left ventricular posterior wall (LVPW) at the level of the papillary muscles. From the M-mode, the left ventricular wall thickness and chamber dimensions were measured. For each mouse, three to five values for each measurement were obtained and averaged for evaluation. The left ventricular (LV) end diastolic dimension (LVEDD), LV end systolic dimension (LVESD), LV septal wall thickness at end diastole (IVSED) and end systole (IVSES), LV posterior wall thickness at end diastole (PWTED) and end systole (PWTES) were measured from a frozen M-mode tracing. Fractional shortening (FS %) is the percent change in LV cavity dimensions. Ejection fraction (EF %) represents stroke volume as a percentage of end diastolic LV volume. The heart rate is automatically determined from the M-mode image by positioning the first and second caliper point on two systolic phases. LV mass is determined automatically by the software or by using the following standard cube function formula: LV mass (mg) = 1.055 [(IVST + LVEDD + PWT)^3 − (LVEDD)^3] (1.055 is the specific gravity of the cardiac muscle).[28] Relative wall thickness (RWT) indicates the overall thickness of the LV wall and is calculated as follows: (RWT) = 2 × PWTD/LVEDD.[28,29]

In Vivo *Blocking of IL-4 and IL-13 during EAM*

Mice were immunized with MyHC$\alpha_{614-629}$ and received 2 mg of rat anti-mouse IL-4 mAb IgG1 clone 11B.11 (American Type Culture Collection) on days −1, 3, 6, 9, 12, 15, and 18. Control mice were injected with isotype control, anti-*Escherichia coli* β-galactosidase mAb IgG1 clone GL113 (kindly provided by Fred Finkelman, University of Cincinnati, Cincinnati, OH). Monoclonal Abs were purified from the concentrated hybridoma supernatants using a HiTrap protein G column (Supelco, Bellefonte, PA). For blocking of IL-13, mice were immunized with MyHC$\alpha_{614-629}$ and injected with 100 μg of αIL-13 mAb rat IgG2b clone 38213 (R&D Systems) on days 0, 4, 8, 12, and 16 of EAM. Normal rat IgG2b clone 141945 (R&D Systems) was used as an isotype control. All Abs were administered in sterile 1× PBS intraperitoneally.

Statistical Analyses

The Mann-Whitney *U*-test was used to compare EAM severity scores between treatment groups. Normally distributed data on continuous parametric axes were analyzed with the two-tailed Student's *t*-test. Values of $P < 0.05$ were considered statistically significant.

Results

IL-13 KO Mice Develop Severe Chronic CVB3-Induced Myocarditis and Heart Failure

We found previously that blockade of IL-4 partially suppresses the development of myosin-induced myocarditis, indicating that IL-4 increases the severity of myocarditis in A/J mice.[9] To investigate the role of another Th2 cytokine, IL-13, in myocarditis, we infected IL-13 KO and WT BALB/c controls with CVB3 and examined hearts for inflammation and viral replication during the early (day 21 after infection) and late phase (day 35 after infection) of chronic myocarditis. We found that IL-13 deficiency significantly increased the severity of chronic CVB3-induced myocarditis at day 35 after infection ($P = 0.001$) (Figure 1A). IL-13 deficiency was also associated with decreased survival. Only 40% of IL-13 KO mice survived past day 21 after infection, whereas none of the WT control mice had died by that time point (Figure 1B). Total IgG autoantibodies against cardiac myosin were also significantly increased in IL-13 KO mice, compared to WT controls ($P < 0.01$) (Figure 1C).

When we examined IL-13 KO mice and WT controls with CVB3-induced myocarditis on day 21 by echocardi-

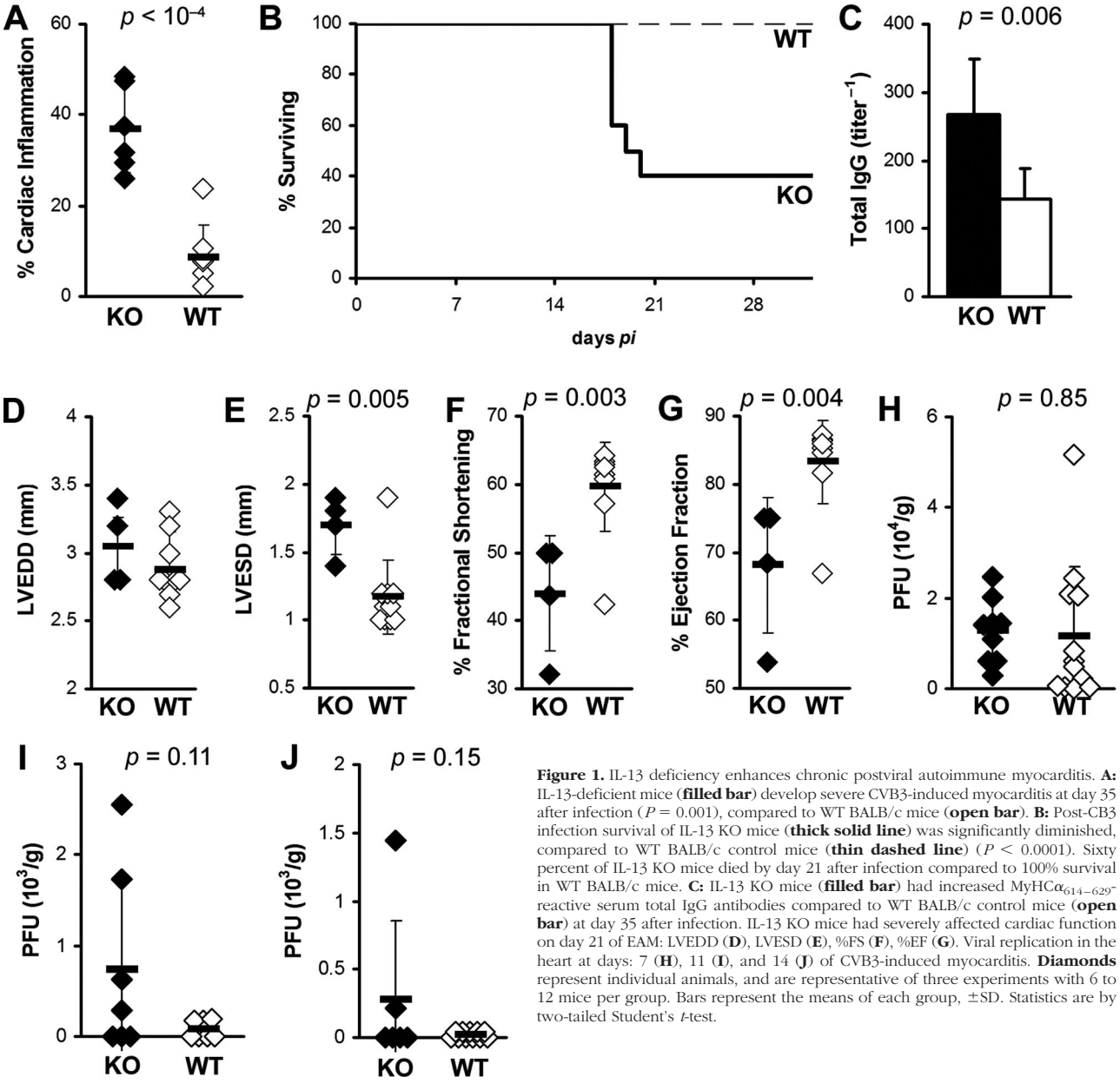

Figure 1. IL-13 deficiency enhances chronic postviral autoimmune myocarditis. **A:** IL-13-deficient mice (**filled bar**) develop severe CVB3-induced myocarditis at day 35 after infection ($P = 0.001$), compared to WT BALB/c mice (**open bar**). **B:** Post-CB3 infection survival of IL-13 KO mice (**thick solid line**) was significantly diminished, compared to WT BALB/c control mice (**thin dashed line**) ($P < 0.0001$). Sixty percent of IL-13 KO mice died by day 21 after infection compared to 100% survival in WT BALB/c mice. **C:** IL-13 KO mice (**filled bar**) had increased MyHC$\alpha_{614-629}$-reactive serum total IgG antibodies compared to WT BALB/c control mice (**open bar**) at day 35 after infection. IL-13 KO mice had severely affected cardiac function on day 21 of EAM: LVEDD (**D**), LVESD (**E**), %FS (**F**), %EF (**G**). Viral replication in the heart at days: 7 (**H**), 11 (**I**), and 14 (**J**) of CVB3-induced myocarditis. **Diamonds** represent individual animals, and are representative of three experiments with 6 to 12 mice per group. Bars represent the means of each group, ±SD. Statistics are by two-tailed Student's *t*-test.

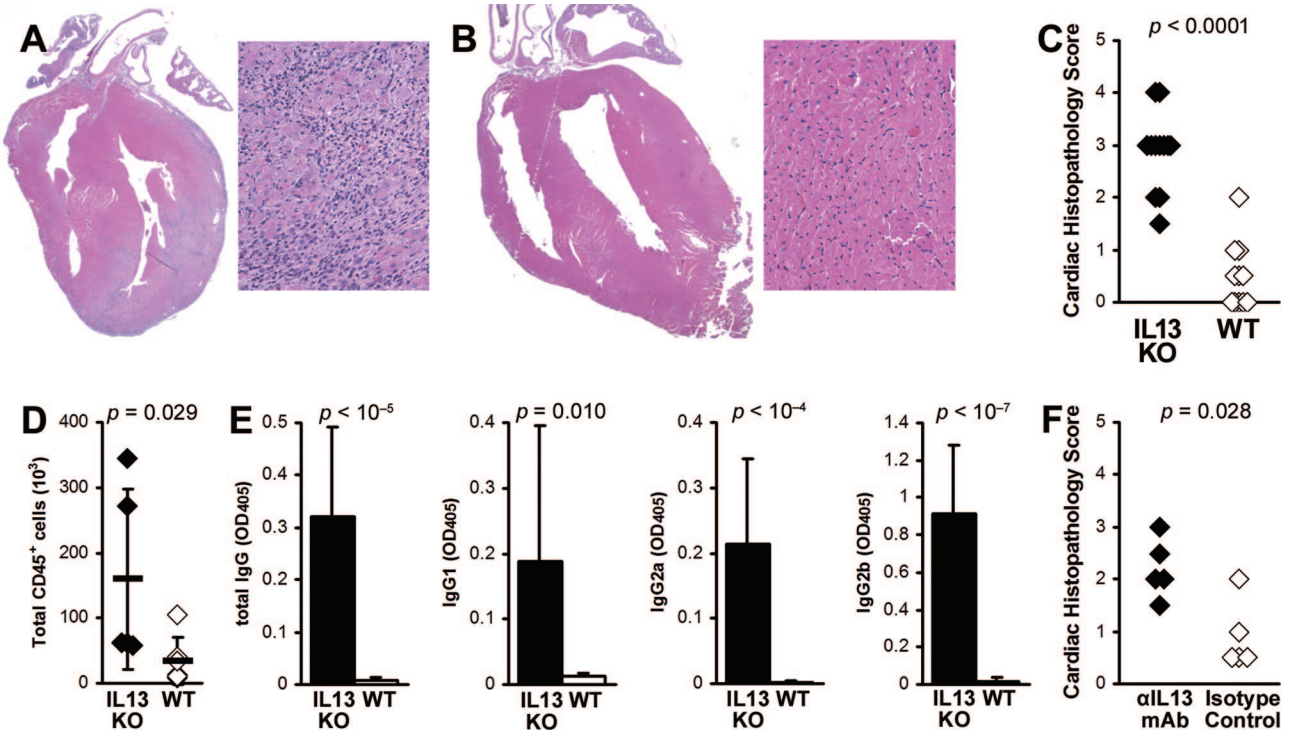

Figure 2. IL-13-deficient mice develop severe myocarditogenic peptide-induced myocarditis. **A:** Representative EAM in an IL-13 KO mouse. **B:** Representative EAM in a WT BALB/c mouse. **C:** The differences in the EAM severity in IL-13 KO mice (**filled diamonds**) were highly significant, compared to WT BALB/c mice (**open diamonds**) at day 21 after infection. Data represent individual animals, and are representative of five repetitions with 8 to 14 mice per group. Statistics are by Mann-Whitney rank sum *U*-test. **D:** Total cardiac-infiltrating $CD45^+$ leukocytes, as calculated by flow cytometry and manual enumeration. **E:** IL-13 KO mice (**filled bars**, $n = 12$) had increased MyHC$\alpha_{614-629}$-reactive serum antibodies compared to WT BALB/c control mice (**open bars**, $n = 11$) at day 21 after infection. Statistics are by two-tailed Student's *t*-test. **F:** Blocking IL-13 with αIL-13 mAb increased severity of EAM, compared to isotype-treated control. Original magnifications: ×5 (**A**, **B**; **left**) and ×64 (**A**, **B**; **right**).

ography, we found significantly compromised cardiac function. IL-13 KO mice that survived to this time point had increased left ventricular end systolic dimension (LVESD) ($P < 0.001$), decreased fractional shortening (%FS) ($P = 0.02$), and decreased ejection fraction (%EF) ($P = 0.05$) (Figure 1, E–G). Left ventricular end diastolic dimension (LVEDD) was not significantly changed at this time point (Figure 1D) although DCM is usually not observed by histology until day 35 after infection. To exclude the possibility that increased viral replication or persistence resulted in increased myocarditis severity; we examined viral replication in IL-13 KO mice at several time points by plaque assay. We found no significant differences in viral replication in the hearts of IL-13 KO mice on day 7 ($P = 0.85$), on day 11 ($P = 0.11$), or on day 14 after infection ($P = 0.15$) (Figure 1, H–J). By day 14, CVB3 was already cleared from most of the WT and IL-13 KO hearts. Viral replication in heart tissue was not detectable at days 21 or 35 in either WT or IL-13 KO mice (data not shown). Thus, IL-13 reduces chronic myocarditis, autoantibody production, and heart failure after viral infection.

Mice Deficient in IL-13 Develop Severe EAM with Increased $CD45^+$ Cardiac-Infiltrating Cells in the Heart

To investigate the role of IL-13 in EAM, we immunized IL-13 KO BALB/c males with the myocarditogenic peptide MyHC$\alpha_{614-629}$ emulsified in CFA.[8] Consistent with the results from CVB3-induced myocarditis, IL-13 deficiency significantly increased the incidence and severity of EAM on day 21 ($P < 0.0001$) (Figure 2, A–C). In EAM hearts, total infiltrating $CD45^+$ cells were significantly increased in IL-13 KO mice (Figure 2D). To test antigen-specific autoantibody responses, we examined the level of MyHC$\alpha_{614-629}$-reactive serum antibodies by ELISA at day 21 of EAM. IL-13 KO mice developed significantly higher levels of MyHC$\alpha_{614-629}$-reactive total IgG, IgG1, IgG2a, and IgG2b, compared to WT mice (Figure 2E). To additionally confirm that IL-13 is protective in EAM, we blocked IL-13 in WT BALB/c mice on days 0, 4, 8, 12, and 16 with anti-IL-13 mAb and also observed increased disease severity at day 21, compared to isotype control-treated mice (Figure 2F). Thus, IL-13 also limits myocarditis in EAM model.

IL-13 KO Mice Have High Levels of Proinflammatory Cytokines and Histamine in Their Hearts

All further studies were done on EAM. To analyze changes in cytokine expression at day 21 of EAM, we homogenized hearts of IL-13 KO and WT control mice and analyzed levels of IFN-γ, IL-1β, IL-4, IL-17, IL-18, TGF-β1, and histamine by ELISA. Th17 cells can mediate severe cardiac pathology when Th1 signaling is disrupt-

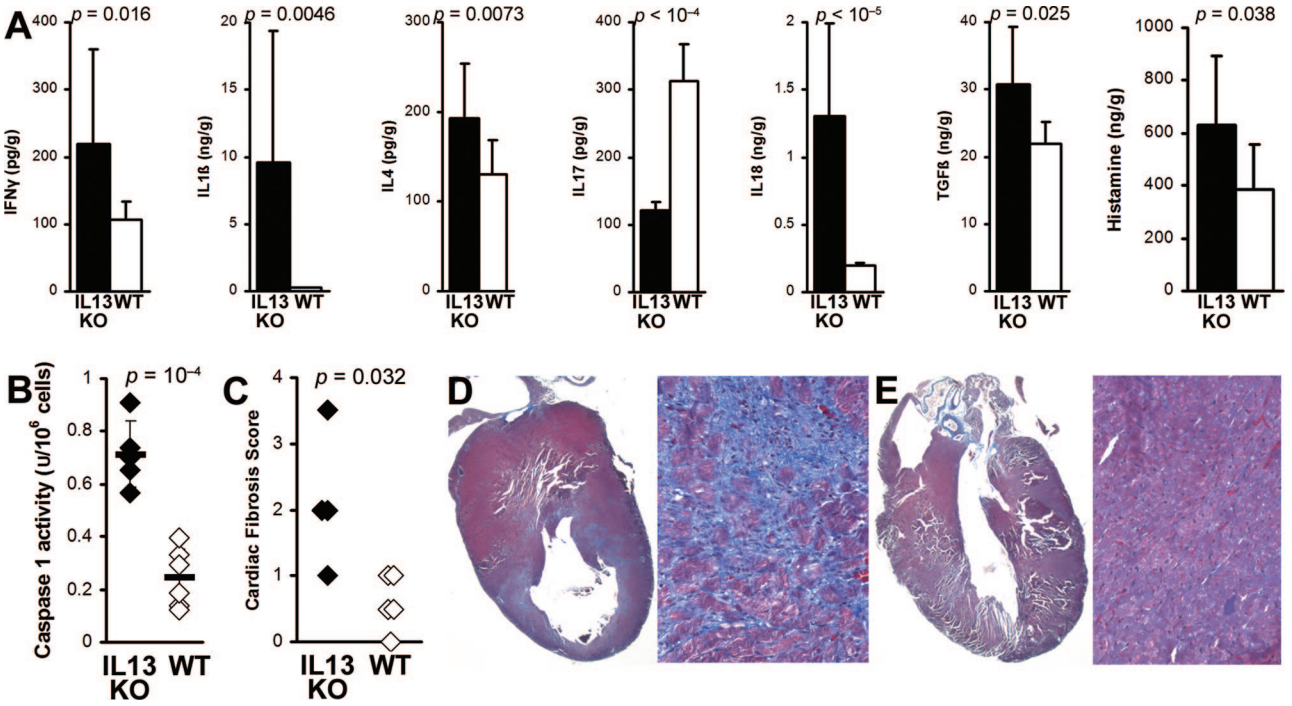

Figure 3. IL-13 KO mice had increased levels of proinflammatory cytokines, histamine, and fibrosis in the heart. **A:** Levels of IFN-γ, IL-1β, IL-4, IL-18, TGF-β1, and histamine from heart homogenates of IL-13 KO mice (**filled bars**, $n = 12$) were significantly higher than in WT BALB/c control mice (**open bars**, $n = 11$) at day 21 after infection of EAM as determined by ELISA. Data represent the means of each group, plus SD, and are normalized to wet heart weight. Statistics are by two-tailed Student's *t*-test. **B:** IL-13 KO (**filled diamonds**) mice had significantly increased caspase-1 activity in splenocytes on day 21 of EAM, compared to WT mice (**open diamonds**). **C:** IL-13 KO mice (**filled diamonds**) develop increased fibrosis on day 30 of EAM compared to WT BALB/c mice (**open diamonds**). Fibrosis was assessed as the area of the heart section with collagen deposition, which stains bright blue with Masson's Trichrome stain. Representative hearts with fibrotic changes in an IL-13 KO mouse (**D**) and WT BALB/c mouse (**E**) are shown.

ed[30,31]; blocking IL-17 with monoclonal antibody decreased myocarditis severity (our unpublished results). Therefore, we measured levels of intracardiac IL-17 to test the hypothesis that Th17 is the driving $CD4^+$ subset mediating increased cardiac pathology in IL-13 KO EAM. However, we found that IL-17 was significantly lower in heart homogenates from IL-13 KO mice at day 21 of EAM, compared to WT BALB/c controls (Figure 3A).

However, we did observe significantly increased levels of IL-1β, IL-18, IFN-γ, TGF-β1, IL-4, and also histamine in the hearts of IL-13 KO mice (Figure 3A). The most markedly increased cytokines were IL-18 and IL-1β; both were increased in hearts as well as in spleens of IL-13 KO mice (data not shown). Pro-IL-18 and pro-IL-1β are converted to their active forms by caspase-1. We found greatly increased caspase-1 activity in IL-13 KO splenocytes on day 21 of EAM ($P = 0.0002$) (Figure 3B). Thus, IL-13 probably protects against myocarditis by down-regulating caspase-1 activity and decreasing levels of active IL-1β and IL-18.

IL-13 KO Mice Have Impaired Cardiac Function in the Chronic Stage of EAM

We have previously shown that fibrosis is associated with progression to DCM and heart failure.[32,33] Although IL-13 is itself associated with fibrosis, its absence does not protect the heart against fibrotic changes caused by other profibrotic cytokines such as TGF-β1, IL-1β, IL-4, and also by histamine (Figure 3A). We have observed increased fibrosis of IL-13 KO mice on day 30 as evaluated by Masson's Trichrome staining for the presence of collagen (Figure 3, C–E). Because IL-13 KO mice had more fibrotic changes in the heart than WT mice, we examined heart function in IL-13 KO mice by echocardiographic imaging the chronic stage of EAM on day 50. IL-13 KO mice demonstrated substantially impaired heart function (Figure 4, A and B), including increased LVEDD ($P = 0.002$) (Figure 4C), increased LVESD ($P < 0.001$) (Figure 4D), decreased %FS ($P < 0.001$) (Figure 4E), and decreased %EF ($P < 0.001$) (Figure 4F). Thus, IL-13 protects against development of severe myocarditis and DCM and cardiac failure in EAM.

EAM Is Not Increased in IL-4 KO BALB/c Mice or after IL-4 Is Blocked with Anti-IL-4 mAb

To examine whether EAM in IL-4 KO mice would resemble EAM in IL-13 KO mice on the BALB/c background, we immunized IL-4 KO and WT BALB/c control mice with myocarditogenic peptide in complete Freund's adjuvant. The severity of myocarditis in IL-4 KO mice on day 21 of EAM, as assessed by histology, was not significantly different compared to WT controls (Figure 5A). No significant differences were observed in intracardiac levels of IL-1β, IL-13, IL-18, or IFN-γ, although there was a tendency toward decreased IL-18 and IL-1β in IL-4 KO mice ($P = 0.059$ and 0.054) (Figure 5B). IL-4 mediates isotype-

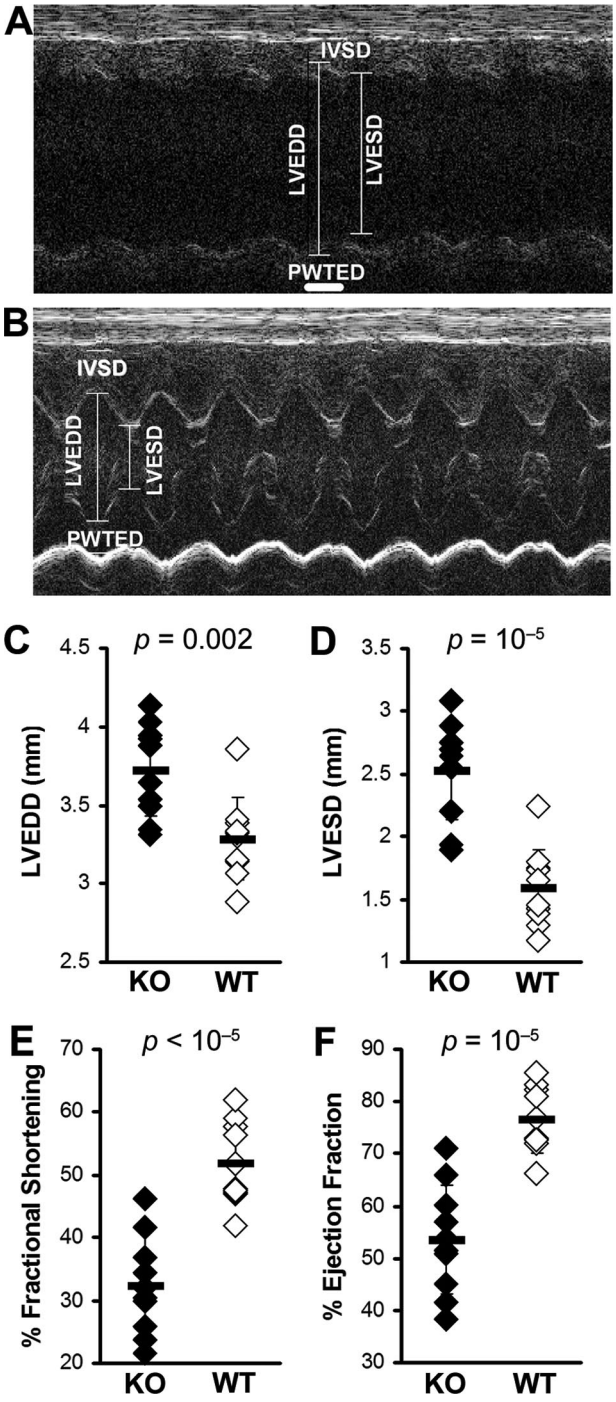

Figure 4. IL-13 KO mice with EAM developed DCM with impaired cardiac function. **A:** Representative M-mode echocardiography of an IL-13 KO mouse at day 50 after infection. **B:** Representative M-mode echocardiography of a WT BALB/c control mouse. The hearts of IL-13 KO mice (**filled bar**, $n = 10$) had significantly increased LVEDD (**C**), LVESD (**D**), and significantly decreased %FS (**E**) and %EF (**F**), compared to WT BALB/c control mice (**open bar**, $n = 10$) at day 50 after infection of EAM.

switching to IgG1[34]; IL-4 KO mice developed low levels of MyHC$\alpha_{614-629}$-reactive IgG1 antibodies, but there was no significant difference compared to WT mice (Figure 5D). IL-4 KO mice had significantly increased levels of MyHC$\alpha_{614-629}$-reactive IgG2a and IgG2b antibodies compared to WT mice ($P < 0.05$) (Figure 5, E and F). Since we have shown previously that blocking of IL-4 with anti-IL-4 mAb in A/J mice decreased disease severity,[9] we blocked IL-4 in WT BALB/c mice with monoclonal antibodies and found no differences in the severity of myocarditis, similar to IL-4 KO mice (Figure 5G). Thus, in contrast to IL-13 deficiency, the absence of IL-4 in BALB/c mice had no significant effect on the severity of myocarditis or the level of proinflammatory cytokines in the heart during EAM.

IL-13/IL-4 Double-Knockout Mice Develop Severe EAM

To examine the interaction of IL-4 and IL-13 in EAM, we induced EAM in IL-13/IL-4 double-knockout (DKO) BALB/c mice. IL-13/IL-4 DKO mice showed significantly increased myocarditis compared to WT BALB/c controls (Figure 6A). IL-13/IL-4 DKO mice developed EAM with comparable histopathological severity to IL-13 KO mice (Figure 2A). Intracardiac IL-18 levels were significantly increased in IL-13/IL-4 DKO mice compared to WT controls (Figure 6B). Also similar to IL-13 KO mice, IL-1β levels were increased in the hearts of some of DKO mice compared to WT BALB/c mice; however, the difference did not reach statistical significance. IL-13/IL-4 DKO mice had no differences in levels of intracardiac IFN-γ and TGF-β1 (Figure 6B). Similar to IL-13 KO mice (Figure 2E), IL-13/IL-4 DKO mice showed significantly higher levels of MyHC$\alpha_{614-629}$-reactive total IgG, IgG2a, and IgG2b antibodies, compared to WT (Figure 6C). In contrast to IL-13 KO mice, the levels of IgG1 were very low in IL-13/IL-4 DKO mice, similar to IL-4 KO mice, because IL-4 is a key cytokine in switching to IgG1.[34] Similar to IL-13 KO mice (Figure 7D), IL-13/IL-4 DKO had decreased $CD4^+CD25^+Foxp3^+$ regulatory T-cell (Treg) populations in spleen (Figure 6D). IL-13/IL-4 DKO mice had a disease phenotype very similar to that of IL-13 KO mice, indicating that IL-13 is a dominant Th2 cytokine in the regulation of EAM in BALB/c mice, compared to IL-4.

Myocarditis in IL-13 KO Mice Is Characterized by Accumulation of T Cells in the Heart and Activation and Increased T-Cell Proliferation and Decreased T Regs in the Spleen of IL-13 KO Mice

EAM in mice has been shown to be predominantly $CD4^+$ T cell-driven.[35,36] Therefore, we examined T-cell populations in IL-13 KO splenocytes with EAM. No differences were observed in the relative proportions of $CD4^+$ or $CD8^+$ T cells in the spleens of IL-13 KO mice when compared to WT mice at day 21 (Supplemental Table 1, see *http://ajp.amjpathol.org*). The effect of IL-13 deficiency on the activation phenotype of T cells *in vivo* was also determined. Flow cytometric analysis of splenic T cells at day 21 demonstrated increased T-cell activation in IL-13 KO mice, as determined by increased proportions of $CD4^+$ and $CD8\alpha^+$ T cells expressing low levels of CD62L (Figure 7A) and high levels of CD28 (Figure 7B)

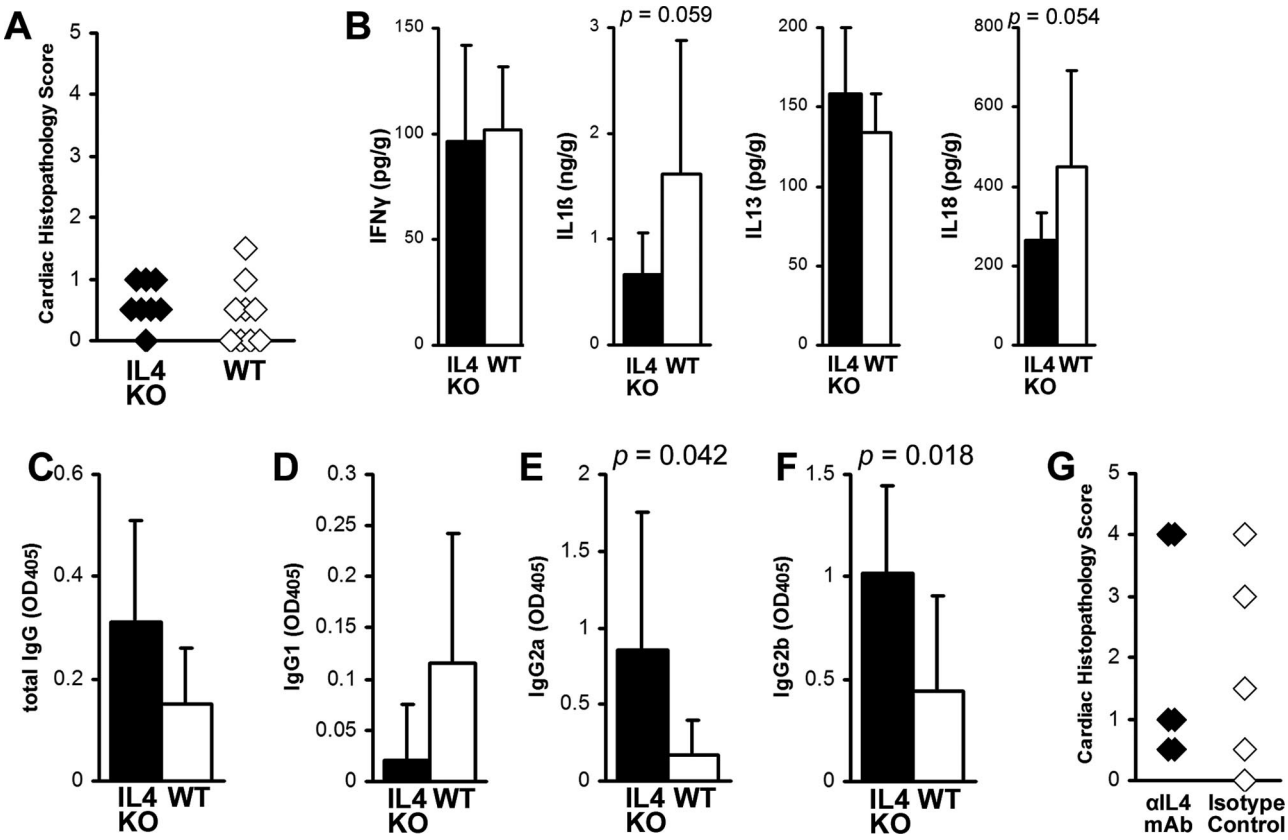

Figure 5. A: IL-4-deficient mice develop mild MyHC$\alpha_{614-629}$-induced myocarditis (**filled diamonds**), comparable to WT BALB/c mice (**open diamonds**). Data represent individual animals, and three repetitions with 8 to 10 mice per group. **B:** There were no differences in levels of intracardiac IL-1β, IL-13, IL-18, or IFN-γ between IL-4 KO (**filled bars**, $n = 8$) and WT BALB/c control mice (**open bars**, $n = 8$) at day 21 after infection of EAM as determined by ELISA. Statistics are by two-tailed Student's t-test. Data are normalized to wet heart weight. MyHC$\alpha_{614-629}$-reactive serum antibodies by subclass: total IgG (**C**), IgG1 (**D**), IgG2a (**E**), IgG2b (**F**). IL-4 KO (**filled bars**, $n = 8$) had higher levels of IgG2a and IgG2b MyHC$\alpha_{614-629}$-reactive serum antibodies than WT BALB/c control mice (**open bars**, $n = 8$) at day 21. **G:** Similar to IL-4 KO mice, we did not observe any differences in EAM severity after treatment with anti-IL-4 mAb, compared to isotype-treated controls. Severity statistics are by Mann-Whitney U-test.

compared to WT mice. Furthermore, spleen cells from IL-13 KO and WT mice with EAM were assessed for antigen-specific proliferation by [^{3}H]methyl-thymidine incorporation. Antigen-specific proliferation of IL-13 KO spleen cells in response to MyHC$\alpha_{614-629}$ was significantly increased in comparison to the specific proliferation of WT BALB/c splenocytes (Figure 7C). To determine whether the severe EAM in the absence of IL-13 was attributable to changes in Treg populations, we examined the proportions of CD4$^+$CD25$^+$Foxp3$^+$ Treg cells in the hearts and spleens of IL-13 KO mice on day 21 of EAM. We did not observe any differences in the proportion of intracardiac Tregs in IL-13 KO mice at this time point (data not shown). In contrast to the heart, a significant decrease in the proportions of CD4$^+$CD25$^+$Foxp3$^+$ Tregs was observed in the spleens of IL-13 KO mice, compared to WT mice on day 21 of EAM ($P = 0.016$) (Figure 7D). To examine T-cell numbers in hearts of IL-13 KO mice, we cannulated the ascending aorta, perfused the hearts with 5% fetal bovine serum in PBS to flush out blood, and then continued perfusion with a digestion buffer containing protease and collagenase to be able to separate infiltrating leukocytes and analyzed the cell suspension by flow cytometry. Both proportional and absolute numbers of CD4$^+$ T cells were substantially increased in IL-13 KO hearts (Figure 7E). Thus, splenic T cells from IL-13 KO mice were more activated and had greater antigen-specific proliferative responses than WT mice but had a decreased T-regulatory T-cell population. Additionally, CD4$^+$ T cells were proportionally as well as absolutely increased in hearts of IL-13 KO mice.

IL-13-Deficient Mice Have Decreased Numbers of Alternatively Activated Macrophages in the Heart

Similar to the observed increase of CD4$^+$ T cells in the hearts of IL-13 KO mice, we also found a significant increase in the numbers of DX5$^+$TCRβ^- NK cells (Tables 1 and 2). Although there were no differences in the proportions of CD19$^+$ B cells or CD8α^+ T cells in the IL-13 KO hearts, absolute numbers of B cells and CD8α^+ T cells were significantly increased (Tables 1 and 2). Surprisingly, although absolute numbers of F4/80$^+$CD11c$^-$ macrophages were increased in IL-13 KO hearts, F4/80$^+$CD11c$^-$ macrophages were proportionally decreased in IL-13 KO hearts. To explain this relative decrease in macrophage numbers that did not correspond to the increase of proinflammatory cytokines in IL-13 KO hearts,

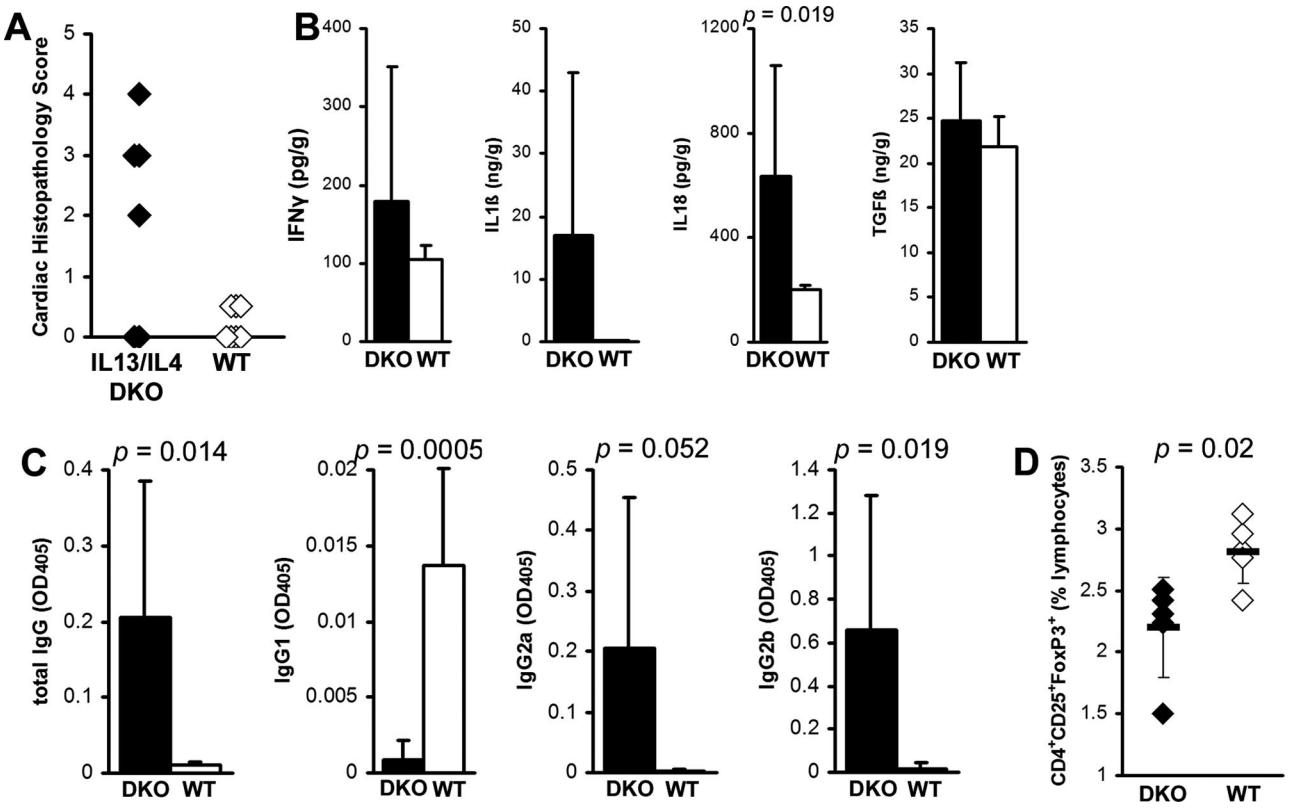

Figure 6. A: IL-13/IL-4 DKO mice (**filled diamonds**) develop myocarditis resembling severe IL-13 KO EAM, which was significantly greater than myocarditis severity in WT BALB/c control mice (**open diamonds**) at day 21 after infection. Data represent individual animals. Individual experiments were conducted five times with 8 to 14 mice per group. **B:** Intracardiac IL-18 was significantly increased in IL-13/IL-4 DKO mice compared to WT BALB/c mice at day 21 after infection of EAM as determined by ELISA. Data are normalized to wet heart weight. **C:** Total IgG MyHC$\alpha_{614-629}$-reactive serum antibodies and its subclasses IgG2a and IgG2b were significantly increased in IL-13/IL-4 DKO (**filled bars**, $n = 8$), compared to WT BALB/c control mice (**open bars**, $n = 8$) at day 21 after infection. IgG1 was significantly decreased in IL-13/IL-4 DKO mice. **D:** $CD4^+CD25^+Foxp3^+$ T cells were decreased in IL-13/IL-4 DKO spleens (**filled diamonds**), compared to WT BALB/c control mice (**open diamonds**) at day 21 of EAM. Statistics are by two-tailed Student's *t*-test.

we further examined the phenotype of monocytes and macrophages in IL-13 KO mice heart infiltrates (Figure 8A). CD204 (macrophage scavenger receptor) and CD206 (macrophage mannose receptor) are markers of alternative activation of macrophages.[23] We observed decreased proportions of double-positive monocytes ($CD11b^{hi}F4/80^-$) bearing both $CD204^+$ and $CD206^+$ in the hearts of IL-13 KO mice at day 21 of EAM (Figure 8B). Moreover, the proportion of mature macrophages ($F4/80^+$) expressing CD204 and/or CD206 was also decreased in IL-13 KO hearts (Figure 8C). On the other hand, we observed strikingly increased proportions of both monocytes and macrophages lacking both CD204 and CD206, which may indicate that classically activated macrophages were increased in hearts of IL-13 KO mice (Figure 8, D and E). These changes were observed in monocyte and macrophage phenotypes when calculated a variety of different ways, whether expressed as proportions of total $CD45^+$ infiltrating leukocytes, as proportions of $CD11b^+F4/80^-$ monocytes or $F4/80^+$ macrophages (data not shown). Taken together, these data indicate that IL-13 has substantial influence over the polarized differentiation of monocyte and macrophage populations in the heart during EAM.

Discussion

We report here that in contrast to IL-4, IL-13 protects against myocarditis in BALB/c mice, whether induced by immunization with cardiac myosin or by viral infection. IL-13 KO mice displayed severe cardiac infiltration involving more than 50% of heart tissue in most mice, resulting in increased fibrosis, cardiac dysfunction, and increased mortality. This severe phenotype contrasts with the mild EAM observed in WT and IL-4 KO mice on the BALB/c background. Overall, these results suggest that IL-13 protects animals from autoimmune myocarditis, independent of IL-4.

The protective effect of IL-13 on myocarditis reported here agrees with the data published by Elnaggar and colleagues,[37] who showed marked amelioration of rat EAM by delivery of an IL-13-Ig fusion gene vector. IL-13 has also been assigned protective roles in other autoimmune diseases. Reduced concentrations of IL-13 are found in the synovium and synovial fluids of rheumatoid arthritis patients.[38] IL-13 was shown to decrease the levels of proinflammatory cytokines and chemokines produced by arthritic synovial tissue *in vitro*, mainly IL-1β, TNF-α, and PGE_2.[39] In a mouse model of collagen-in-

duced arthritis, IL-13 decreased the severity of arthritis by reducing TNF-α and IL-1β levels, and reducing the total number of monocytes, lymphocytes, and polymorphonuclear cells in the joint. IL-13 treatment decreased arthritis when used either before or after disease induction.[40] Human recombinant (hr) IL-13 has a protective effect in a rat model of experimental autoimmune encephalomyelitis, with decreased clinical and histological signs of disease.[41] In the NOD mouse model of diabetes, hrIL-13 was shown to prevent insulitis and diabetes.[42] Thus, IL-13 can be protective in several other autoimmune disease models.

In our study, the absence of IL-13 resulted in severe autoimmune myocarditis in both the viral model and EAM, progressing to DCM, cardiac dysfunction, and heart failure. We were unable to detect any significant differences in viral replication on days 7, 11, or 14 after infection in IL-13 KO mouse hearts, compared to WT mice. However, in some of the experiments, we have observed a nonsignificant tendency toward increased viral replication in IL-13 KO mice, although the difference never reached significance. Virus was undetectable at days 21 or 35 in both IL-13 KO and WT mice.

In the absence of virus, EAM in IL-13-deficient animals was associated with substantially increased $CD45^+$ leukocyte infiltration of the heart; the absolute numbers of most immune cell types were increased at day 21 after infection. By day 30, much of the infiltration was replaced by severe fibrosis in IL-13 KO mice. We have previously shown that fibrosis is associated with progression to DCM and heart failure in both EAM and CVB3-induced myocarditis.[32,43] IL-1β, IL-4, TGF-β1, and histamine are known to induce fibrosis,[32,44,45] and were increased in IL-13 KO mice, which may account for the greater production of collagen by day 30 of EAM. In IL-13 KO mice increased fibrosis led to DCM with cardiac dysfunction and heart failure, as observed by echocardiographic imaging and decreased survival of IL-13 KO mice. Thus, IL-13 limits inflammation during myocarditis, and thereby protects against the development of fibrosis, DCM, and heart failure.

We observed up-regulation of both cellular and humoral adaptive immune responses in IL-13 KO mice. We observed increased absolute numbers of intracardiac $CD19^+$ B cells and increased anti-myosin antibody production in IL-13 KO mice. T-cell responses were affected at multiple levels. In the absence of IL-13, activation of spleen $CD4^+$ and $CD8\alpha^+$ T cells increased, as did antigen-specific proliferation of splenocytes. Absolute, as well as proportional numbers of intracardiac $CD4^+$ T cells

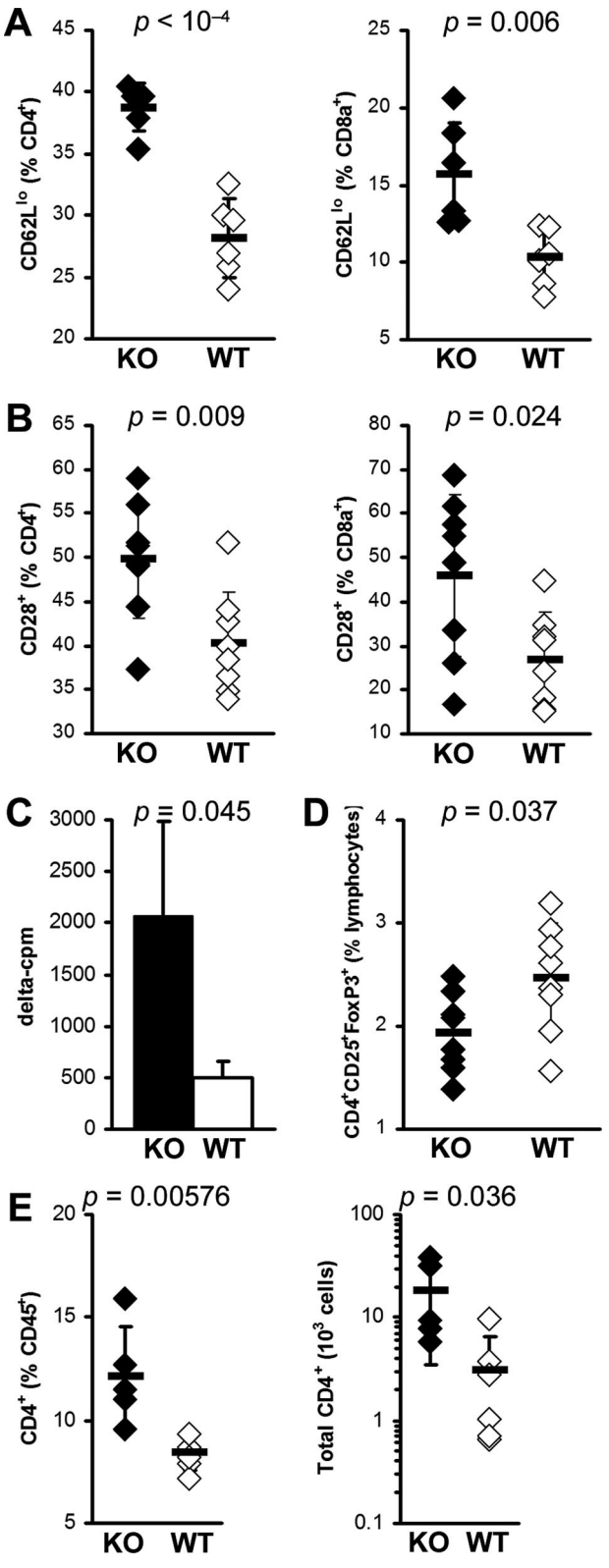

Figure 7. IL-13 KO mice display greater spleen T-cell activation. **A:** Activated $CD4^+$ (**left**) and $CD8\alpha^+$ (**right**) T cells were determined by surface $CD62L^{lo}$ expression. **B:** Activated $CD4^+$ (**left**) and $CD8\alpha^+$ (**right**) T cells were determined by surface CD28 expression. Data represent percentage of $CD4^+$ or $CD8\alpha^+$-gated cells in individual IL-13 KO (**filled diamonds**) or WT (**open diamonds**) animals. Horizontal bars indicate the mean of each group ± the SD. Data are representative of two independent experiments. **C:** Seventy-two-hour proliferation of spleen cells from IL-13 KO mice (**filled bar**) is greater than from WT BALB/c mice (**open bar**) in response to 10 μg/ml of $MyHC\alpha_{614-629}$ at day 21 after infection, as determined by [^{3}H]Me-thymidine uptake. Data indicate the mean δ cpm (stimulated cpm − unstimulated cpm; values for individual animals are the mean of triplicate wells) for each group ($n = 3$); plus the SD. **D:** $CD4^+CD25^+Foxp3^+$ Treg cells as a proportion of spleen lymphoid cells, in IL-13 KO (**filled diamonds**) or WT (**open diamonds**) animals at day 21 after infection. **E:** Intracardiac $CD4^+$ T cells as a proportion of total $CD45^+$ leukocytes (**left**) and calculated absolute numbers (**right**) in IL-13 KO (**filled diamonds**) or WT (**open diamonds**) animals at day 21 after infection. Horizontal bars indicate the mean of each group ± the SD. Statistics are by two-tailed Student's *t*-test.

Table 1. Cardiac-Infiltrating Leukocyte Populations in EAM in IL-13 KO Mice, Expressed as a Proportion of Gated $CD45^+$ Leukocytes

Population (%$CD45^+$)	KO	WT	*P*
$CD8\alpha^+$ T cells	4.18 ± 0.76%	3.43 ± 1.05%	0.22
$CD4^+$ T cells	12.1 ± 2.4%	8.4 ± 0.8%	0.00576
$CD19^+Mac3^-$ B cells	13.6 ± 4.5%	13.1 ± 2.8%	0.85
$F4/80^+CD11c^-$ macrophages	10.8 ± 3.5%	16.6 ± 4.4%	0.0388
$CD11c^{hi}$ dendritic cells	21.1 ± 7.2%	21.9 ± 6.5%	0.85
$CD117^+Fc\epsilon RI\alpha^+$ mast cells	9.42 ± 1.96%	12.08 ± 3.61%	0.18
$CXCR2^+Gr1^+$ neutrophils	3.82 ± 2.28%	4.83 ± 2.22%	0.47
$DX5^+TCR\beta^-$ NK cells	5.94 ± 0.67%	3.33 ± 0.65%	0.00011
$DX5^+TCR\beta^+$ NKT cells	1.26 ± 0.48%	0.98 ± 0.42%	0.33

Intracardiac leukocytes from perfused, digested hearts of each genotype ($n \geq 5$) at day 21 of disease were stained and analyzed by flow cytometry. Numbers represent mean ± SD. Statistics are by two-tailed Student's *t*-test.

were increased in the hearts of IL-13 KO mice. We considered the possibility that the expansion or induction of $CD4^+CD25^+Foxp3^+$ Treg may be decreased in IL-13 KO EAM. Skapenko and colleagues[46] showed that IL-13 is important in the extrathymic development of Tregs in an antigen-dependent manner. Although we did not observe a difference in the proportion of intracardiac Tregs on day 21 of EAM, we found significantly decreased numbers of $CD4^+CD25^+Foxp3^+$ Tregs in the spleens of both IL-13 KO and IL-4/IL-13 DKO mice. This decrease of Tregs in the spleen suggests that IL-13 may be important in the induction or maintenance of Treg populations in the spleen, but it is not clear that it contributed to the protective effect of IL-13 in myocarditis.

IL-13 did not appear to protect against myocarditis by deviating Th1/Th2 responses. Guo and colleagues[47] showed that T cells from IL-13 KO mice had decreased capacity to produce IL-4 *in vitro*, compared to WT mice. However, we have shown here that IL-13 KO mice have significantly increased levels of intracardiac IL-4 as well as IL-5 (data not shown) and increased levels of $MyHC\alpha_{614-629}$-specific IgG1, indicating that IL-13 KO mice are able to generate Th2 responses. This is in agreement with a report from McKenzie and colleagues[48] that showed that the defective Th2 responses in IL-13 KO mice are not readily apparent *in vivo*. Furthermore, IFN-γ and IgG2a levels, markers of a Th1 response, were increased in IL-13 KO mice. Thus, responses associated with both Th1 and Th2 immunity were up-regulated in the absence of IL-13. Strikingly, we observed that IL-4 KO mice developed a very different disease phenotype from that of IL-13 KO mice. Previously, we have blocked IL-4 in A/J mice by mAb and observed decreased EAM severity.[9] Here, we observed that IL-4 KO mice on the BALB/c background developed mild myocarditis comparable to WT BALB/c mice on day 21. Blockade of IL-4 in WT BALB/c mice did not change the severity of myocarditis compared to isotype controls.

We are currently backcrossing the IL-4 KO allele to the A/J background to be able to address whether these observed differences are attributable to different background genetics in A/J and BALB/c mice. Although we did not observe statistically significant changes in myocarditis severity in IL-4 KO BALB/c mice, there was some indication that IL-4 may contribute to the pathogenesis of myocarditis because levels of intracardiac IL-1β and IL-18 tended to be lower in IL-4 KO mice. We had previously shown that both of these proinflammatory cytokines are important in myocarditogenesis; levels of IL-1β in the heart correlate well with histopathological assessment of disease severity.[49,50] IL-4/IL-13 DKO mice developed severe cardiac infiltration, increased autoantibody responses, increased proinflammatory cytokines, and decreased Tregs in spleen—comparable with disease in IL-13 KO animals, suggesting a dominant role of IL-13 over IL-4 in disease pathogenesis. To help confirm the protective role of IL-13 in myocarditis, we also blocked IL-13 by mAb and observed a significant increase in myocarditis severity, compared to isotype controls, consistent with the knockout. Myocarditis in αIL-13-treated animals was not as severe as in IL-13 KO mice, presumably because of incomplete neutralization of IL-13.

A novel Th subset, Th17, has been shown to be pathogenic in several autoimmune disease models.[51–53] It was

Table 2. Cardiac-Infiltrating Leukocyte Populations in EAM in IL-13 KO Mice, Expressed as Absolute Numbers

Population (10^3 cells)	KO	WT	*P*
$CD8\alpha^+$ T cells	6.3 ± 5.0	1.1 ± 1.2	0.035
$CD4^+$ T cells	18.4 ± 15.0	3.1 ± 3.5	0.036
$CD19^+Mac3^-$ B cells	17.3 ± 10.3	4.5 ± 5.0	0.024
$F4/80^+CD11c^-$ macrophages	15.8 ± 12.7	4.7 ± 3.3	0.066
$CD11c^{hi}$ dendritic cells	36.7 ± 37.5	9.0 ± 12.7	0.122
$CD117^+Fc\epsilon RI\alpha^+$ mast cells	15.7 ± 14.3	3.8 ± 4.2	0.082
$CXCR2^+Gr1^+$ neutrophils	8.4 ± 9.7	2.1 ± 2.8	0.160
$DX5^+TCR\beta^-$ NK cells	9.7 ± 8.5	1.0 ± 0.8	0.033
$DX5^+TCR\beta^+$ NKT cells	1.9 ± 1.8	0.24 ± 0.16	0.052

Absolute values were calculated by multiplying percent $CD45^+$ values (Table 1) by enumerative cell counts of viable, noncardiomyocyte cells by Trypan Blue exclusion hemocytometry. Numbers represent mean ± SD. Statistics are by two-tailed Student's *t*-test.

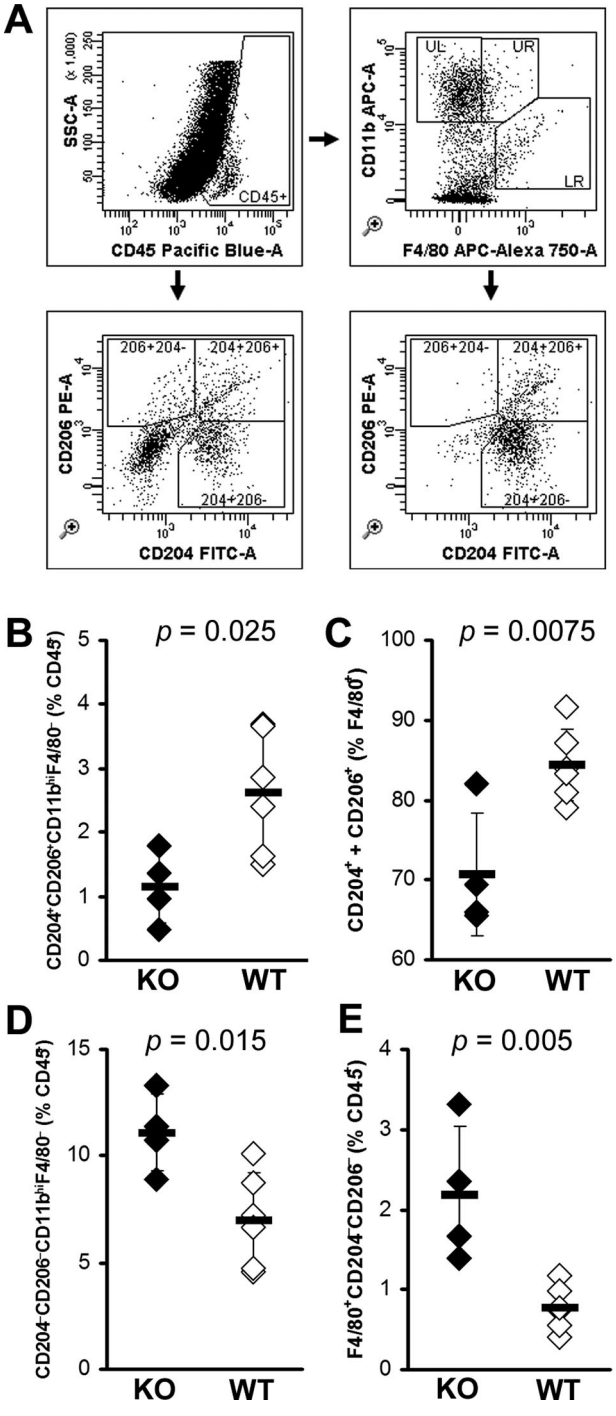

Figure 8. Monocyte and macrophage phenotypes in the hearts of IL-13 KO mice at day 21 of EAM. **A:** Representative gating of intracardiac monocyte and macrophage populations. Infiltrating $CD45^+$ leukocytes are subsetted by bivariate analysis of F4/80 and CD11b expression, revealing distinct populations: UL, $CD11b^{hi}F4/80^-$ monocytes; UR, $CD11b^{hi}F4/80^{int}$ macrophages; LR, $F4/80^{hi}CD11b^{int}$ macrophages. CD204 and CD206 expression are then determined, based on gates set from total $CD45^+$ cells. **B:** $CD204^+CD206^+$ double-positive expression on $CD11b^{hi}F4/80^-$ monocytes, as a proportion of $CD45^+$ cells. **C:** $CD204^+$ or $CD206^+$ expression, as a proportion of total $F4/80^+$ macrophages. $CD204^-CD206^-$ double-negative $CD11b^{hi}F4/80^-$ monocytes (**D**) and $F4/80^+$ macrophages (**E**), as a proportion of total $CD45^+$ cells. Individual IL-13 KO (**filled**) and WT (**open**) animals are shown. Horizontal bars indicate the mean of each group ± the SD. Statistics are by two-tailed Student's *t*-test.

recently proposed that pathology in EAM is driven by IL-17-producing $CD4^+$ T cells because severe myocarditis in *T-bet* KO mice was associated with increased IL-17 in the heart.[30] We have found that blocking IL-17 significantly ameliorates EAM (unpublished observations); therefore, Th17 is an important pathway for the pathogenesis of myocarditis. However, we found decreased levels of IL-17 in the hearts and spleens (data not shown) of IL-13 KO mice, suggesting that Th17 $CD4^+$ T cells are not responsible for increased inflammation in the absence of IL-13. Thus, this severe form of disease in IL-13 KO mice cannot be explained by enhanced IL-17 production. Clearly, the pathogenesis of myocarditis can be driven by multiple mechanisms.

Rather than deviating Th1/Th2 differentiation or increasing IL-17 production, IL-13 instead appears to down-regulate the production of proinflammatory cytokines in EAM. Although both B and T cells appear up-regulated in the absence of IL-13, the IL-13 receptor, IL-13Rα1, is not expressed on mouse T or B cells.[54] Therefore, IL-13 has no direct signaling effects on mouse T and B cells and the change we observed is likely attributable to their regulation by other cell types that are dependent on IL-13. One possibility is that a major target for IL-13 is the innate immune system; by down-regulating the innate immune response, IL-13 may also down-regulate subsequent adaptive immune responses.

Potential targets for IL-13 include mast cells, natural killer (NK) cells, and dendritic cells. We observed increased proportions of NK cells and mast cells in the spleen and significantly increased numbers of NK cells and significantly increased histamine levels in the hearts of IL-13 KO mice on day 21 of EAM. However, macrophages are a primary source of IL-1β and IL-18, and are a major component of the heart infiltrate during both myosin- and CVB3-induced myocarditis.[26,37] It was shown that monocytes incubated with IL-13 up-regulated or down-regulated 142 different genes.[22] Some of these changes in gene regulation reflect the fact that IL-13 is able to increase the number of alternatively activated macrophages. Activation of macrophages in the presence of IL-4 or IL-13 induces expression of arginase-1, the mannose receptor (CD206), and the type A scavenger receptor (CD204).[23] We have observed increases in the absolute numbers of macrophages in the heart infiltrate but proportionally compared to other components of the infiltrate, macrophages were decreased in hearts of IL-13 KO mice. We have found that the decrease is attributable to a reduction of $CD206^+$ or $CD204^+$ monocytes and macrophages that represent the alternatively activated subset, whereas the $CD204^-CD206^-$ monocyte and macrophage populations were increased in the hearts of IL-13 KO mice. Thus, IL-13 deficiency is associated with an increase of classically activated macrophages in the heart and a decrease of alternatively activated macrophages.

One important group of genes that have been shown to be regulated by IL-13 in monocytes included several components of regulation of IL1, such as IL-1 receptor antagonist (IL-1ra) and caspase-1.[22] We did not observe any differences in intracardiac production of IL-1ra in

IL-13 KO mice (data not shown).[55] Classically activated macrophages are a major source of proinflammatory cytokines, including IL-1. Caspase-1 is a key enzyme in converting IL-18 and IL-1β to their active forms, and we observed striking up-regulation of caspase-1 enzymatic activity on day 21 of EAM in splenocytes of IL-13 KO mice. This increased caspase-1 activity is likely responsible for increased levels of IL-1β and IL-18 in the absence of IL-13, corresponding with a shift in macrophage populations toward classically activated macrophages in the heart of IL-13 KO mice. These data might predict that alternatively activated macrophages mediate protection from disease, or that classically activated macrophages are a major pathophysiological effector in myocarditis.

Thus, IL-13 may limit the activation of effector T cells indirectly by altering activation, differentiation, proliferation, or survival of cells and proximal mediators of the innate autoimmune response. Most markedly, IL-13 protects against myocarditis by its multiple effects on monocytes and macrophages.

Acknowledgments

We thank Andrew N.J. McKenzie from the Medical Research Council Laboratory of Molecular Biology, Cambridge, UK, for providing IL-13 KO and IL-13/IL-4 DKO mice; Tonya Wells and the laboratories of Dr. Jonathan Schneck for help with paramagnetic cell selection; R. Lee Blosser and Ada Tam for expert assistance with flow cytometric acquisition and analysis; and Dr. Patrizio Caturegli for valuable comments.

References

1. Rose NR, Afanasyeva M: The inflammatory process in experimental myocarditis. Inflammation and Cardiac Diseases. Edited by Feuerstein GZ, Libby P, Mann DL. Basel, Birkhauser Verlag 2003, pp 325–333
2. Carniel E, Sinagra G, Bussani R, Di Lenarda A, Pinamonti B, Lardieri G, Silvestri F: Fatal myocarditis: morphologic and clinical features. Ital Heart J 2004, 5:702–706
3. Fairweather D, Afanasyeva M, Rose NR: Cellular immunity: a role for cytokines. The Heart in Systemic Autoimmune Diseases. Edited by Doria A, Pauletto P. Amsterdam, Elsevier 2004, pp 3–17
4. Fairweather D, Rose NR: Inflammatory heart disease: a role for cytokines. Lupus 2005, 14:646–651
5. Neu N, Beisel KW, Traystman MD, Rose NR, Craig SW: Autoantibodies specific for the cardiac myosin isoform are found in mice susceptible to Coxsackievirus B3-induced myocarditis. J Immunol 1987, 138:2488–2492
6. Neu N, Craig SW, Rose NR, Alvarez F, Beisel KW: Coxsackievirus induced myocarditis in mice: cardiac myosin autoantibodies do not cross-react with the virus. Clin Exp Immunol 1987, 69:566–574
7. Neu N, Rose NR, Beisel KW, Herskowitz A, Gurri-Glass G, Craig SW: Cardiac myosin induces myocarditis in genetically predisposed mice. J Immunol 1987, 139:3630–3636
8. Pummerer CL, Luze K, Grassl G, Bachmaier K, Offner F, Burrell SK, Lenz DM, Zamborelli TJ, Penninger JM, Neu N: Identification of cardiac myosin peptides capable of inducing autoimmune myocarditis in BALB/c mice. J Clin Invest 1996, 97:2057–2062
9. Afanasyeva M, Wang Y, Kaya Z, Park S, Zilliox MJ, Schofield BH, Hill SL, Rose NR: Experimental autoimmune myocarditis in A/J mice is an interleukin-4-dependent disease with a Th2 phenotype. Am J Pathol 2001, 159:193–203
10. Fairweather D, Rose NR: Coxsackievirus-induced myocarditis in mice: a model of autoimmune disease for studying immunotoxicity. Methods 2007, 41:118–122
11. de Vries JE: The role of IL-13 and its receptor in allergy and inflammatory responses. J Allergy Clin Immunol 1998, 102:165–169
12. Reiman RM, Thompson RW, Feng CG, Hari D, Knight R, Cheever AW, Rosenberg HF, Wynn TA: Interleukin-5 (IL-5) augments the progression of liver fibrosis by regulating IL-13 activity. Infect Immun 2006, 74:1471–1479
13. Wills-Karp M: Interleukin-13 in asthma pathogenesis. Immunol Rev 2004, 202:175–190
14. Fichtner-Feigl S, Strober W, Kawakami K, Puri RK, Kitani A: IL-13 signaling through the IL-13alpha2 receptor is involved in induction of TGF-beta1 production and fibrosis. Nat Med 2006, 12:99–106
15. McKenzie GJ, Bancroft A, Grencis RK, McKenzie AN: A distinct role for interleukin-13 in Th2-cell-mediated immune responses. Curr Biol 1998, 8:339–342
16. Bancroft AJ, McKenzie AN, Grencis RK: A critical role for IL-13 in resistance to intestinal nematode infection. J Immunol 1998, 160:3453–3461
17. Fallon PG, Richardson EJ, McKenzie GJ, McKenzie AN: Schistosome infection of transgenic mice defines distinct and contrasting pathogenic roles for IL-4 and IL-13: IL-13 is a profibrotic agent. J Immunol 2000, 164:2585–2591
18. McKenzie GJ, Fallon PG, Emson CL, Grencis RK, McKenzie AN: Simultaneous disruption of interleukin (IL)-4 and IL-13 defines individual roles in T helper cell type 2-mediated responses. J Exp Med 1999, 189:1565–1572
19. Zhu Z, Homer RJ, Wang Z, Chen Q, Geba GP, Wang J, Zhang Y, Elias JA: Pulmonary expression of interleukin-13 causes inflammation, mucus hypersecretion, subepithelial fibrosis, physiologic abnormalities, and eotaxin production. J Clin Invest 1999, 103:779–788
20. Whittaker L, Niu N, Temann UA, Stoddard A, Flavell RA, Ray A, Homer RJ, Cohn L: Interleukin-13 mediates a fundamental pathway for airway epithelial mucus induced by CD4 T cells and interleukin-9. Am J Respir Cell Mol Biol 2002, 27:593–602
21. Terabe M, Matsui S, Noben-Trauth N, Chen H, Watson C, Donaldson DD, Carbone DP, Paul WE, Berzofsky JA: NKT cell-mediated repression of tumor immunosurveillance by IL-13 and the IL-4R-STAT6 pathway. Nat Immunol 2000, 1:515–520
22. Scotton CJ, Martinez FO, Smelt MJ, Sironi M, Locati M, Mantovani A, Sozzani S: Transcriptional profiling reveals complex regulation of the monocyte IL-1 beta system by IL-13. J Immunol 2005, 174:834–845
23. Gordon S: Alternative activation of macrophages. Nat Rev Immunol 2003, 3:23–35
24. Eriksson U, Kurrer MO, Sonderegger I, Iezzi G, Tafuri A, Hunziker L, Suzuki S, Bachmaier K, Bingisser RM, Penninger JM, Kopf M: Activation of dendritic cells through the interleukin 1 receptor 1 is critical for the induction of autoimmune myocarditis. J Exp Med 2003, 197:323–331
25. Afanasyeva M, Georgakopoulos D, Belardi DF, Ramsundar AC, Barin JG, Kass DA, Rose NR: Quantitative analysis of myocardial inflammation by flow cytometry in murine autoimmune myocarditis: correlation with cardiac function. Am J Pathol 2004, 164:807–815
26. Fairweather D, Frisancho-Kiss S, Yusung SA, Barrett MA, Davis SE, Steele RA, Gatewood SJ, Rose NR: IL-12 protects against coxsackievirus B3-induced myocarditis by increasing IFN-gamma and macrophage and neutrophil populations in the heart. J Immunol 2005, 174:261–269
27. Olson LE, Bedja D, Alvey SJ, Cardounel AJ, Gabrielson KL, Reeves RH: Protection from doxorubicin-induced cardiac toxicity in mice with a null allele of carbonyl reductase 1. Cancer Res 2003, 63:6602–6606
28. Yang XP, Liu YH, Rhaleb NE, Kurihara N, Kim HE, Carretero OA: Echocardiographic assessment of cardiac function in conscious and anesthetized mice. Am J Physiol 1999, 277:H1967–H1974
29. Basset A, Blanc J, Messas E, Hagege A, Elghozi JL: Renin-angiotensin system contribution to cardiac hypertrophy in experimental hyperthyroidism: an echocardiographic study. J Cardiovasc Pharmacol 2001, 37:163–172
30. Rangachari M, Mauermann N, Marty RR, Dirnhofer S, Kurrer MO, Komnenovic V, Penninger JM, Eriksson U: T-bet negatively regulates autoimmune myocarditis by suppressing local production of interleukin 17. J Exp Med 2006, 203:2009–2019
31. Marty RR, Eriksson U: Dendritic cells and autoimmune heart failure. Int J Cardiol 2006, 112:34–39

32. Fairweather D, Frisancho-Kiss S, Yusung SA, Barrett MA, Davis SE, Gatewood SJ, Njoku DB, Rose NR: Interferon-gamma protects against chronic viral myocarditis by reducing mast cell degranulation, fibrosis, and the profibrotic cytokines transforming growth factor-beta 1, interleukin-1 beta, and interleukin-4 in the heart. Am J Pathol 2004, 165:1883–1894
33. Afanasyeva M, Georgakopoulos D, Belardi DF, Bedja D, Fairweather D, Wang Y, Kaya Z, Gabrielson KL, Rodriguez ER, Caturegli P, Kass DA, Rose NR: Impaired up-regulation of CD25 on CD4+ T cells in IFN-gamma knockout mice is associated with progression of myocarditis to heart failure. Proc Natl Acad Sci USA 2005, 102:180–185
34. Bergstedt-Lindqvist S, Moon HB, Persson U, Moller G, Heusser C, Severinson E: Interleukin 4 instructs uncommitted B lymphocytes to switch to IgG1 and IgE. Eur J Immunol 1988, 18:1073–1077
35. Smith SC, Allen PM: The role of T cells in myosin-induced autoimmune myocarditis. Clin Immunol Immunopathol 1993, 68:100–106
36. Eriksson U, Ricci R, Hunziker L, Kurrer MO, Oudit GY, Watts TH, Sonderegger I, Bachmaier K, Kopf M, Penninger JM: Dendritic cell-induced autoimmune heart failure requires cooperation between adaptive and innate immunity. Nat Med 2003, 9:1484–1490
37. Elnaggar R, Hanawa H, Liu H, Yoshida T, Hayashi M, Watanabe R, Abe S, Toba K, Yoshida K, Chang H, Minagawa S, Okura Y, Kato K, Kodama M, Maruyama H, Miyazaki J, Aizawa Y: The effect of hydrodynamics-based delivery of an IL-13-Ig fusion gene for experimental autoimmune myocarditis in rats and its possible mechanism. Eur J Immunol 2005, 35:1995–2005
38. Woods JM, Haines GK, Shah MR, Rayan G, Koch AE: Low-level production of interleukin-13 in synovial fluid and tissue from patients with arthritis. Clin Immunol Immunopathol 1997, 85:210–220
39. Woods JM, Katschke KJ Jr, Tokuhira M, Kurata H, Arai KI, Campbell PL, Koch AE: Reduction of inflammatory cytokines and prostaglandin E2 by IL-13 gene therapy in rheumatoid arthritis synovium. J Immunol 2000, 165:2755–2763
40. Woods JM, Amin MA, Katschke KJ Jr, Volin MV, Ruth JH, Connors MA, Woodruff DC, Kurata H, Arai K, Haines GK III, Kumar P, Koch AE: Interleukin-13 gene therapy reduces inflammation, vascularization, and bony destruction in rat adjuvant-induced arthritis. Hum Gene Ther 2002, 13:381–393
41. Cash E, Minty A, Ferrara P, Caput D, Fradelizi D, Rott O: Macrophage-inactivating IL-13 suppresses experimental autoimmune encephalomyelitis in rats. J Immunol 1994, 153:4258–4267
42. Zaccone P, Phillips J, Conget I, Gomis R, Haskins K, Minty A, Bendtzen K, Cooke A, Nicoletti F: Interleukin-13 prevents autoimmune diabetes in NOD mice. Diabetes 1999, 48:1522–1528
43. Afanasyeva M, Georgakopoulos D, Fairweather D, Caturegli P, Kass DA, Rose NR: Novel model of constrictive pericarditis associated with autoimmune heart disease in interferon-gamma-knockout mice. Circulation 2004, 110:2910–2917
44. Manabe I, Shindo T, Nagai R: Gene expression in fibroblasts and fibrosis: involvement in cardiac hypertrophy. Circ Res 2002, 91:1103–1113
45. Kuwahara F, Kai H, Tokuda K, Kai M, Takeshita A, Egashira K, Imaizumi T: Transforming growth factor-beta function blocking prevents myocardial fibrosis and diastolic dysfunction in pressure-overloaded rats. Circulation 2002, 106:130–135
46. Skapenko A, Kalden JR, Lipsky PE, Schulze-Koops H: The IL-4 receptor alpha-chain-binding cytokines. IL-4 and IL-13, induce forkhead box P3-expressing CD25+CD4+ regulatory T cells from CD25−CD4+ precursors. J Immunol 2005, 175:6107–6116
47. Guo L, Hu-Li J, Zhu J, Pannetier C, Watson C, McKenzie GJ, McKenzie AN, Paul WE: Disrupting Il13 impairs production of IL-4 specified by the linked allele. Nat Immunol 2001, 2:461–466
48. McKenzie GJ, Emson CL, Bell SE, Anderson S, Fallon P, Zurawski G, Murray R, Grencis R, McKenzie AN: Impaired development of Th2 cells in IL-13-deficient mice. Immunity 1998, 9:423–432
49. Fairweather D, Yusung S, Frisancho S, Barrett M, Gatewood S, Steele R, Rose NR: IL-12 receptor beta 1 and Toll-like receptor 4 increase IL-1 beta- and IL-18-associated myocarditis and coxsackievirus replication. J Immunol 2003, 170:4731–4737
50. Lane JR, Neumann DA, Lafond-Walker A, Herskowitz A, Rose NR: Role of IL-1 and tumor necrosis factor in Coxsackie virus-induced autoimmune myocarditis. J Immunol 1993, 151:1682–1690
51. Koenders MI, Lubberts E, van de Loo FA, Oppers-Walgreen B, van den Bersselaar L, Helsen MM, Kolls JK, Di Padova FE, Joosten LA, van den Berg WB: Interleukin-17 acts independently of TNF-alpha under arthritic conditions. J Immunol 2006, 176:6262–6269
52. Komiyama Y, Nakae S, Matsuki T, Nambu A, Ishigame H, Kakuta S, Sudo K, Iwakura Y: IL-17 plays an important role in the development of experimental autoimmune encephalomyelitis. J Immunol 2006, 177:566–573
53. Yen D, Cheung J, Scheerens H, Poulet F, McClanahan T, McKenzie B, Kleinschek MA, Owyang A, Mattson J, Blumenschein W, Murphy E, Sathe M, Cua DJ, Kastelein RA, Rennick D: IL-23 is essential for T cell-mediated colitis and promotes inflammation via IL-17 and IL-6. J Clin Invest 2006, 116:1310–1316
54. de Vries JE, Zurawski G: Immunoregulatory properties of IL-13: its potential role in atopic disease. Int Arch Allergy Immunol 1995, 106:175–179
55. de Waal Malefyt R, Figdor CG, Huijbens R, Mohan-Peterson S, Bennett B, Culpepper J, Dang W, Zurawski G, de Vries JE: Effects of IL-13 on phenotype, cytokine production, and cytotoxic function of human monocytes. Comparison with IL-4 and modulation by IFN-gamma or IL-10. J Immunol 1993, 151:6370–6381